 CMES, vol.6, no.5, pp.441-451, 2004

2D Incompressible Viscous Flows at Moderate and High Reynolds Numbers

Alfredo Nicolás[1] **and Blanca Bermúdez**[2]

Abstract: 2D incompressible vicous flows from the unsteady Navier-Stokes equations in stream function-vorticity variables are presented. The results are obtained using a simple numerical procedure based on a fixed point iterative process to solve the nonlinear elliptic system that results once a second order time discretization is performed. Flows on the unregularized unit driven cavity are reported up to Reynolds numbers Re=5000 to compare them with those reported by other authors and supposed to be correct. Various long time computations are presented for Re=10000 to see its evolution as time-dependent flow. Moreover, results are reported for $Re = 10000$, $Re = 15000$ and $Re = 20000$ to see how their flow looks like close from its departure $t = 0$; with these kind of results transition to turbulence is observed as time or Reynolds number increases because of the increment of new small structures (subvortices or eddies).

1 Introduction

The main goal of this short paper is to present 2D incompressible viscous flows from the unsteady Navier-Stokes equations in stream function-vorticity variables. These flows are obtained applying a numerical procedure based mainly on a fixed point iterative process, extended to the boundary, to solve the nonlinear elliptic system that results once a convenient second order time discretization is made. The iterative process leads to the solution of, uncoupled, well-conditioned, symmetric linear elliptic problems for which very efficient solvers exist either by finite differences or finite elements as far as rectangular domains are considered.

Flows on the unregularized unit driven cavity are reported to validate the numerical procedure up to Reynolds numbers Re=5000 with those of Goyon (1996) for the unsteady problem, where a different method is used in the same stream function-vorticity formulation and the same boundary conditions work out here; the validation is reinforced comparing some results with the ones in Schreiber and Keller (1983) from the steady problem in terms also of such formulation.

Beyond the validation just mentioned, the capability of the numerical procedure for handling *high* Reynolds numbers is described. Various long time computations for Re=10000 are shown to illustrate the evolution as *time-dependent* flow; with this specific case we go further on the discussion in Goyon (1996), and Pan and Glowinski (2000) that for high Reynolds numbers the flow is time-dependent (supposed to be so for Reynolds numbers > 7500). For higher Reynolds numbers (up to $Re = 20000$) we show results at the beginning of the flow based on the fact that the numerical procedure has the ability to start directly from the initial condition at $t = 0$ and not necessarily from a smaller Reynolds number previously calculated.

Unlike the numerical scheme in Bermúdez and Nicolás (1999), where very coarse meshes are used since an upwinding effect is taken into account, here no upwinding ingredient is considered. Then, the meshes for the results of this work follow the size dictated by the thickness of the boundary layer (of order of $Re^{-1/2}$); furthermore, no refining on the mesh is required near the boundary.

Among recent meshless methods related with this work we can mention Lin and Atluri (2001) and Tsai et al. (2202). In the former, the steady-state incompressible Navier-Stokes equations are studied in its general primitive variables formulation (general in the sense that, unlike the stream function-vorticity variables, 3D problems can be tackled). To satisfy the un-avoidable incompressibility constraint, the standard mixed formulation is modified by adding approximate "perturbation" terms based on residual forms of the Euler-Lagrange equations to the local weak formulation of such constraint. Despite the 3D generality of the Meshless Local Petrov-Galerkin numerical scheme and the appropriate upwinding scheme

[1] Depto. Matemáticas, 3er. Piso Ed. Diego Bricio, UAM-Iztapalapa, 09340 México D.F. México, e-mail: anc@xanum.uam.mx

[2] Facultad de C. de la Computación, BUAP, Pue., México, e-mail: bbj@solarium.cs.buap.mx

to stabilize convection dominated problems that are considered, the numerical experiments, so far, involve only 2D problems at moderate Reynolds numbers. In the latter, a Meshless BEM method is developed to solve 3D Stokes flows in terms of the velocity-vorticity formulation which is the 3D version of the 2D stream function-vorticity one. Surprisingly, the iterative process used is very close to ours, the only difference is that ours is a truly fixed point one and a different time discretization is used. Actually, Tsai et al. claim that their method can be extended to the 3D velocity-vorticity Navier-Stokes equations and it seems that ours too. However, we can not guarantee in advance the same 2D performance since the 3D Navier-Stokes problem is very different; a new non trivial term appears: the term that gives rise to a phenomenon referred to as *vortex stretching* (Doering and Gibbon, 1995, p. 10)

In Section 2 the problem is formulated, in Section 3 the numerical procedure is described, the numerical experiments appear in Section 4 and in Section 5 some conclusions are made. On Section 4 we proceed as follows: 1) For $Re = 400$ a kind of mesh convergence is presented showing some velocity profiles on three different meshes and then show the vorticity contours and streamlines, from the optimal of these meshes, to compare them with those in Schreiber and Keller (1983) obtained from the steady problem; next, flows for $Re = 1000$ and $Re = 5000$ are compared with the ones in Schreiber an Keller and/or in Goyon (1996). 2) Various long time computations are presented for $Re = 10000$. They show that the flow is time-dependent; one of these results shows that at time $T = 275$ the flow almost passes over the steady one of Schreiber and Keller, and then it changes as time goes on. 3) Results for $Re = 10000, 15000, 20000$ at the beginnig of the flow are shown to see how the number of subvortices (or "eddies") increases as the Reynolds number grows and, at least for $Re = 10000$, how the number of them increases as time increases; both situations laying like in transition to turbulence (Landau and Lifshitz, 1989).

Even though the meshes for high Reynolds numbers seemed to be finer than usual[3], considerably finer than the ones in Lin and Atluri (2001) and in Bermúdez and Nicolás (1999), there is not too much computational effort based on the well conditioning of the resultant algebraic linear systems, which are solved efficiently with iterative methods in medium computers. About stability, the time step Δt ranges from 0.01 for moderate Reynolds numbers to 0.0025 for high ones (this latter value being a natural demand to capture the fast dynamics of the flows due to small viscosities). For $Re = 400$ the right result can be obtained with a time step bigger than 0.01 but the number of iterations of the fixed point process increases in such a way that computing time is worse. This situation is a constant for the Reynolds numbers studied so far. For the results reported, we have chosen the reasonable time step no less than most unsteady numerical procedures use, for instance $\Delta t = 0.0025$ is used in Goyon's work for $Re = 10000$.

[3] $\frac{1}{256} \times \frac{1}{256}, \frac{1}{384} \times \frac{1}{384}, \frac{1}{512} \times \frac{1}{512}$ for $Re = 10000, 15000$ and 20000 respectively

2 The Navier-Stokes equations

Let $\Omega \subset R^2$ be the region of the flow of an unsteady incompressible viscous fluid, and Γ its boundary. This kind of flow may be modeled by the following Navier-Stokes equations in terms of the stream function-vorticity variables

$$\begin{cases} \Delta\psi = \omega \ in \ \Omega, \ t > 0 \ \ (a) \\ \omega_t - \nu\Delta\omega + \mathbf{u}\cdot\nabla\omega = 0 \ in \ \Omega, \ t > 0, \ (b) \end{cases} \tag{1}$$

where the velocity $\mathbf{u} = (u_1, u_2)$ (primitive variable) and the stream function ψ are related by

$$\begin{cases} u_1 = \frac{\partial\psi}{\partial y}, \quad u_2 = -\frac{\partial\psi}{\partial x}, \end{cases} \tag{2}$$

and the vorticity ω by

$$\omega = \frac{\partial u_1}{\partial y} - \frac{\partial u_2}{\partial x}; \tag{3}$$

the viscosity parameter ν is given by $\nu = \frac{1}{Re}$, with Re denoting the Reynolds number.

This work is only concerned with the well known, unregularized unit driven cavity problem which implies recirculation phenomena because of its velocity boundary condition; then, equations (1) are set in the domain $\Omega = (0,1) \times (0,1)$ and the boundary condition, in terms of the primitive variable $\mathbf{u}$, is defined by $\mathbf{u} = (1,0)$ at the moving boundary (the top one) and $\mathbf{u} = (0,0)$ elsewhere.

By (2), ψ is a constant function on solid and fixed walls; at the moving wall $y = 1$, a constant function for ψ is also

obtained. Then, following Goyon (1996), $\psi = 0$ is chosen on Γ. As mentioned in Dean, Glowinski and Pironneau (1991) and in Peyret and Taylor (1983), ψ is overdetermined on the boundary ($\frac{\partial \psi}{\partial n}|_\Gamma$ is also known) and no boundary condition is given for ω; to overcome this difficulty various alternatives have been proposed (see, for instance Dean et al. and Peyret and Taylor just mentioned). This work follows the alternative for rectangular domains given by Goyon (1996); thus, by Taylor expansions of $(1a)$ on the boundary, with h_x and h_y as the space steps, and considering $h_x = h_y = h$ for the driven cavity under study, the following $O(h^2)$ relations are obtained

$$\left\{\begin{array}{l} \omega(0,y,t) = \frac{1}{2h^2}[8\psi(h,y,t) - \psi(2h,y,t)] \\ \omega(1,y,t) = \frac{1}{2h^2}[8\psi(1-h,y,t) - \\ \psi(1-2h,y,t)] \\ \omega(x,0,t) = \frac{1}{2h^2}[8\psi(x,h,t) - \psi(x,2h,t)] \\ \omega(x,1,t) = \frac{1}{2h^2}[8\psi(x,1-h,t) - \\ \psi(x,1-2h,t)] + \frac{3}{h} \end{array}\right. \tag{4}$$

For the sake of completeness, Taylor expansion (omitting the time variable t) for $\psi(x,1-h)$ and $\psi(x,1-2h)$ gives

$$\frac{\partial^2 \psi}{\partial y^2}(x,1) = \frac{1}{2h^2}[8\psi(x,1-h) - \psi(x,1-2h)] - \frac{7}{2h^2}\psi(x,1) + \frac{3}{h}\frac{\partial \psi}{\partial y}(x,1) + O(h^2). \tag{5}$$

Noting that $\psi(x,1) = 0$, $\frac{\partial \psi}{\partial y}(x,1) = 1$ and $\frac{\partial^2 \psi}{\partial x^2}(x,1) = 0$, then, taking back the time variable, (5) implies $\omega(x,1,t) = \Delta\psi(x,1,t) = \frac{1}{2h^2}[8\psi(x,1-h,t) - \psi(x,1-2h,t)] + \frac{3}{h} + O(h^2)$.

In addition, $\omega(\mathbf{x},0) = \omega_0(\mathbf{x})$ denotes the initial condition for the vorticity which, by (3), has to satisfy $\omega_0 = \frac{\partial u_{01}}{\partial y} - \frac{\partial u_{02}}{x}$ if $\mathbf{u_0} = (u_{01}, u_{02})$ is the initial velocity.

3 Numerical procedure

About the time discretization, for the time derivative appearing in the vorticity equation (1.b) the following well known second-order approximation is used

$$\omega_t(\mathbf{x}, n\Delta t) = \frac{3\omega^{n+1} - 4\omega^n + \omega^{n-1}}{2\Delta t}, \ \mathbf{x}\varepsilon\Omega, \tag{6}$$

where $n \geq 1$, Δt denotes the time step and $\omega^r \equiv \omega(\mathbf{x}, r\Delta t)$. The resulting time discretization system reads

$$\left\{\begin{array}{l} \Delta\psi^{n+1} = \omega^{n+1}, \\ \alpha\omega^{n+1} - \nu\Delta\omega^{n+1} + \mathbf{u}^{n+1}\cdot\nabla\omega^{n+1} = f_\omega, \end{array}\right. \tag{7}$$

where $\alpha = \frac{3}{2\Delta t}$, $f_\omega = \frac{4\omega^n - \omega^{n-1}}{2\Delta t}$; the components u_1 and u_2 of $\mathbf{u}$, in terms of ψ, are given by (2).

Then, at each time step, a nonlinear system of elliptic equations of the following form has to be solved

$$\left\{\begin{array}{l} \Delta\psi = \omega \ \ in \ \ \Omega, \\ \psi = 0 \quad on \ \ \Gamma; \\ \alpha\omega - \nu\Delta\omega + \mathbf{u}\cdot\nabla\omega = f \ \ in \ \ \Omega, \\ \omega = \omega_{bc} \ \ on \ \ \Gamma. \end{array}\right. \tag{8}$$

To obtain (ψ^1, ω^1) in (7), an Euler first-order approximation is applied for the time derivative through a subsequence with a smaller time step to keep up with second-order accuracy; a system of the form (8) is also obtained.

Taking into account that the elliptic system (8), in addition to be nonlinear, is of non-potential (or transport) type, a fixed point iterative process is used to solve it. This process is similar to one applied to thermal problems, in connection with mixed convection in primitive variables, Bermúdez and Nicolás (1999). A distinctive aspect here is that the iterative process is extended until the boundary to handle the ω boundary conditions given implicitly by interior values of ψ in (4).

Denoting $R(\omega,\psi) \equiv \alpha\omega - \nu\Delta\omega + \mathbf{u}\cdot\nabla\omega - f \ \ in \ \Omega$; then, system (8) is equivalent to

$$\left\{\begin{array}{l} \Delta\psi = \omega \ \ in \ \ \Omega, \qquad \psi = 0 \ \ on \ \ \Gamma, \\ R(\omega,\psi) = 0 \ \ in \ \ \Omega, \ \ \omega = \omega_{bc} \ \ on \ \ \Gamma. \end{array}\right. \tag{9}$$

Then, (9) is solved, at the time level $(n+1)$, by the fixed point iterative process:

With $\omega^0 = \omega^n$ given, until convergence on ω solve

$$\left\{\begin{array}{l} \Delta\psi^{m+1} = \omega^m \ \ in \ \ \Omega, \ \psi^{m+1} = 0 \ \ on \ \ \Gamma; \\ \\ \omega^{m+1} = \omega^m - \rho(\alpha I - \nu\Delta)^{-1} \\ R(\omega^m, \psi^{m+1}) \ \ in \ \ \Omega, \ \rho > 0, \\ \\ \omega^{m+1} = \omega_{bc}^{m+1} \ \ on \ \ \Gamma; \end{array}\right. \tag{10}$$

and then, take $(\omega^{n+1}, \psi^{n+1}) = (\omega^{m+1}, \psi^{m+1})$.

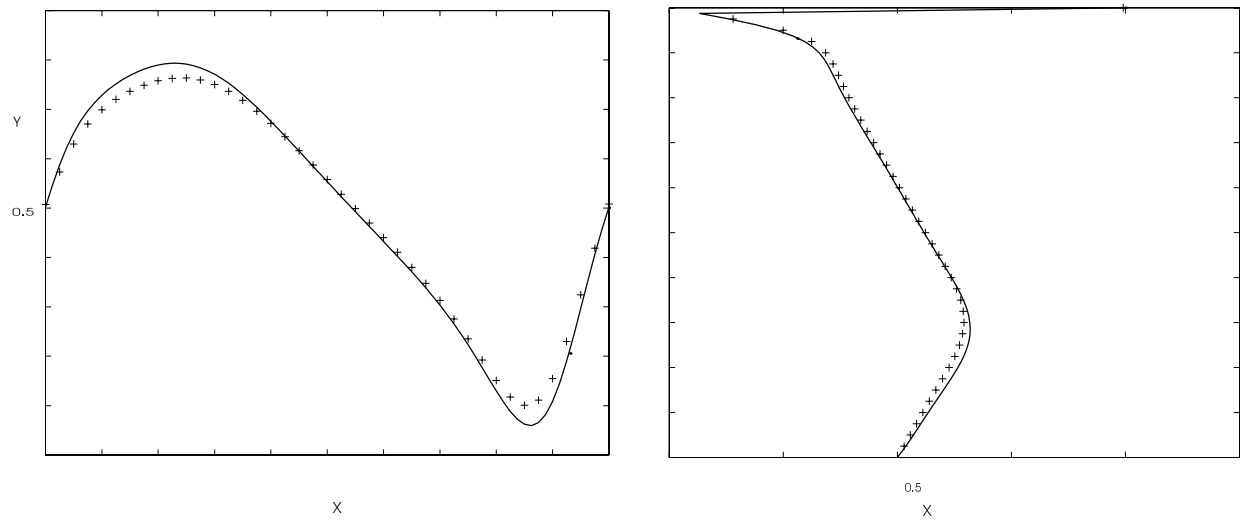

Figure 1 : Re=400; perfiles at y=0.5 (left) and at x=0.5 (right): h=1/40 (+), h=1/80 (continuous), h=1/160 (...)

Finally, system (10) is equivalent to

$$\begin{cases} \Delta\psi^{m+1} = \omega^m \quad in \quad \Omega,\ \psi^{m+1} = 0 \ \ on \ \ \Gamma; \\ (\alpha I - \nu\Delta)\omega^{m+1} = (\alpha I - \nu\Delta)\omega^m \\ \qquad\qquad -\rho R(\omega^m, \psi^{m+1}) \ in \ \ \Omega, \\ \omega^{m+1} = \omega_{bc}^{m+1} \ \ on \ \ \Gamma. \end{cases} \tag{11}$$

It turns out that at each iteration *two uncoupled* elliptic linear problems associated to the operators Δ and $\alpha I - \nu\Delta$ are solved; it should be noted that the non-symmetric part for ω has been taken to the right hand side thanks to the iterative process. Therefore, the solution of the original system, at each iteration of each time level, leads to the solution of standard symmetric linear elliptic problems.

It is well known that for the space discretization of elliptic problems like those in (11), either finite differences or finite elements may be used, as far as rectangular domains are concerned; it is also known that in either case very efficient solvers exist. In the finite element case, variational formulations have to be chosen and then restrict them to the finite dimensional finite elements spaces, for instance like those in Gunzburger (1989), Dean, Glowinski and Pironneau (1991) and Glowinski (2003). For the specific results in the following Section 4, the second order approximation of the Fishpack solver (Adams, Swarztrauber and Sweet, 1980) has been used, where the algebraic linear systems are solved through an efficient cyclic reduction iterative method (Sweet, 1977); then, such second order approximation in space combined with the second order one for vorticity boundary conditions (4) and the second order approximation in time (6) imply that the whole approximate problem is based on second order discretizations.

4 Numerical experiments

In the experiments that follow $\Delta t = 0.01$ for Reynolds numbers from $Re = 400$ to $Re = 5000$ and $\Delta t = 0.0025$ for higher ones; h denotes the space step size.

1). The results for $Re = 400, 1000, 5000$ correspond to the asymptotic steady state obtained from the solution of the non-steady problem. $Re = 1000$ and $Re = 5000$ are compared with the ones in Goyon (1996); and $Re = 400$ and $Re = 1000$ are compared with those in Schreiber and Keller (1983).

Figure 1 shows the profiles at $y = 0.5$ (left) and $x = 0.5$ (right) for $Re = 400$ on three diferent meshes: $h = 1/40, 1/80, 1/160$. It is observed that there is good agreement for the last two. Then, we choose $h = 1/80$ as the optimal one (the coarse one to give the accuracy required). We reinforce this choice showing in Figure 2 the corresponding vorticity contours (left) and the streamlines (right) which agree perfectly with the ones in Schreiber and Keller (1983). Based on this kind of mesh independence, for larger Reynolds numbers we choose the right mesh as the one that gives the vorticity contours and streamlines reported by other authors to be correct.

Figure 3 shows the vorticity contours and the streamlines for $Re = 1000$ with $h = 1/120$ and Figure 4 the corresponding profiles at $y = 0.5$ and $x = 0.5$; both, con-

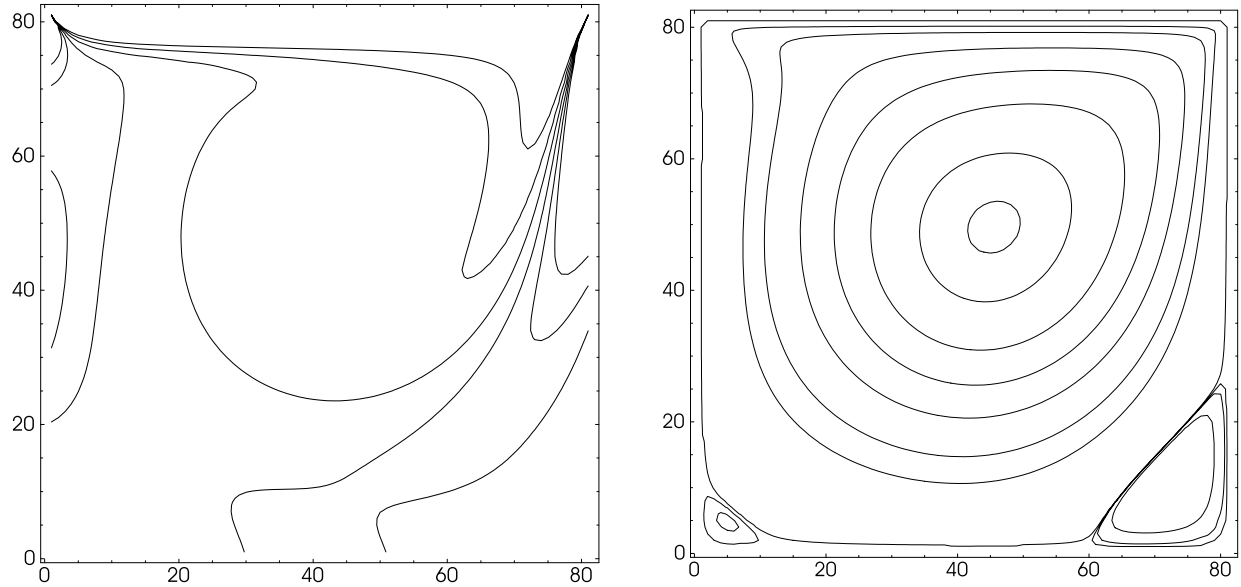

Figure 2 : Re=400 (vs S. & Keller)

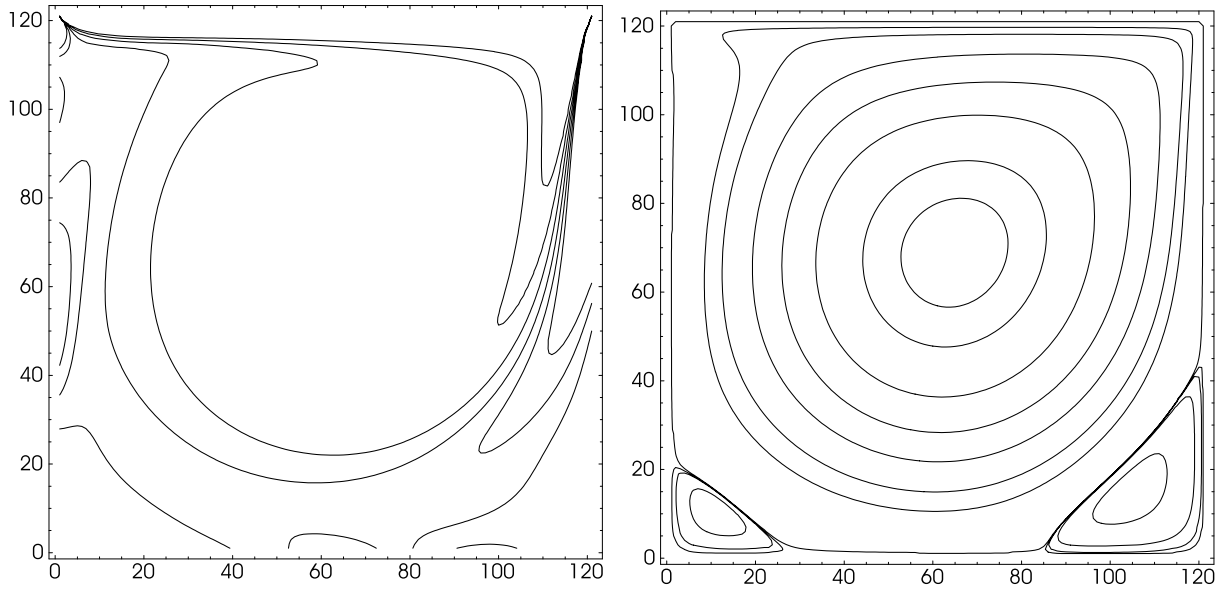

Figure 3 : Re=1000 (vs S. & Keller)

tours and profiles agree with the ones in Schreiber and Keller (they do not show profiles for $Re = 400$). Figure 5 shows the corresponding contours for $Re = 1000$ but this time with the contour values given by Goyon (1996). In both cases the vorticity fails to be correct if a bigger h is used. Goyon obtains this result with $h = 1/128$; then ours is a bit better, and much better our previous result for $Re = 400$ obtained with $h = 1/80$ since Goyon does not show $Re = 400$ but shows $Re = 100$ with $h = 1/128$. Figura 6 shows the corresponding vorticity contours and streamlines for $Re = 5000$ with $h = 1/256$, same h as in Goyon, and they agree with the ones in Goyon.

2). A set of results follows, with $h = 1/256$ and $\Delta t = 0.0025$, for $Re = 10000$ to illustrate the evolution as time-dependent flow (like before, vorticity contours are the left ones and stream lines the right ones).

Figure 7 shows the flow at $T = 275$ and it is observed that it almost reaches the Schreiber and Keller result from the

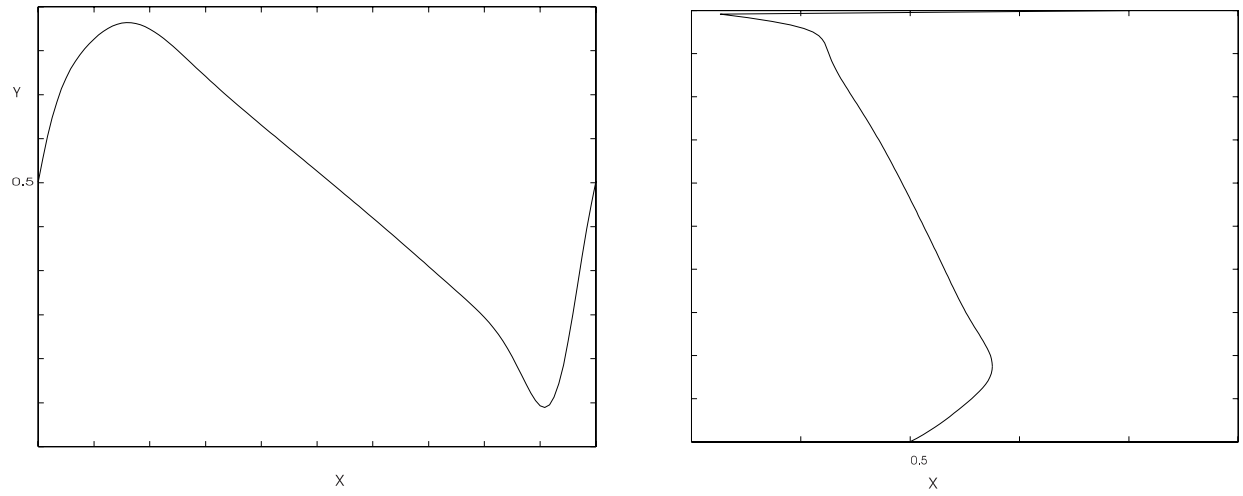

Figure 4 : Re=1000 (vs S. & Keller)

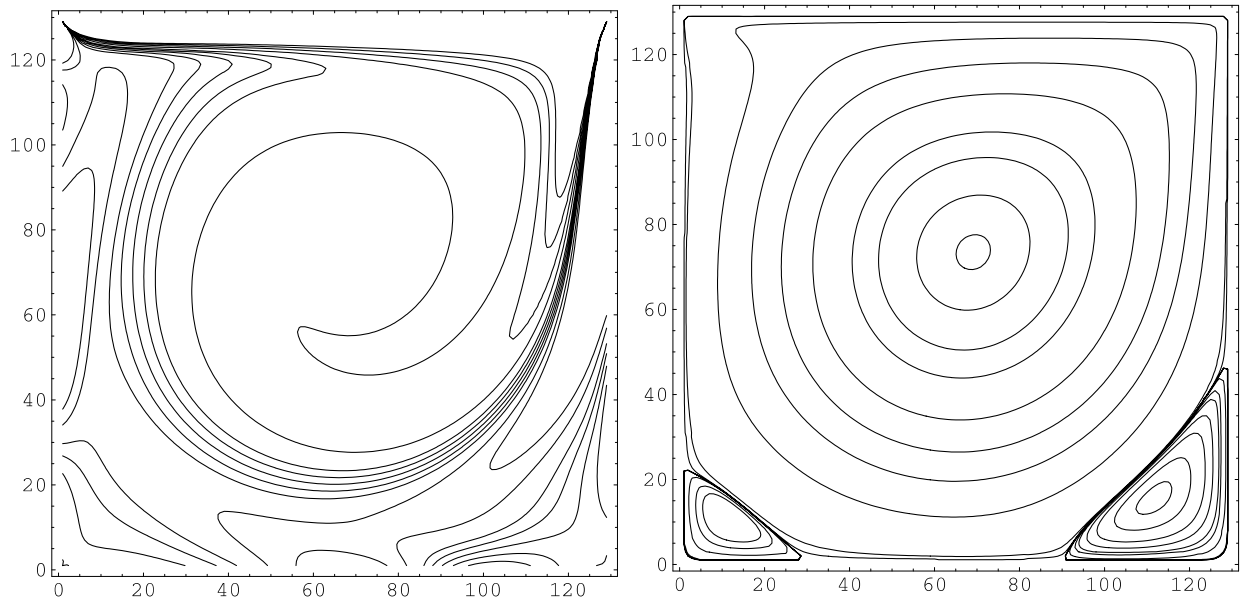

Figure 5 : Re=1000 (vs Goyon)

steady problem. This "almost" means that the streamlines agree very well, but, to have all the contour structures for the vorticity up to some small distortion mainly on the upstream top corner, the contour values ± 5. (two out of six) have to be moved to ± 5.62. For this case, Figure 8 shows the profiles at $y = 0.5$ (left) and $x = 0.5$ (right); the profiles in Schreiber and Keller out of the boundary layer look almost straight while ours look a little bit curved, due possibly to the movement of two vorticity contour values and the small distortion mentioned. In conclusion we could say that this flow is not reaching exactly the state given by the steady problem and it may be seen as a first indication to be a time-dependent flow.

Figures 9 and 10 show the flow at final times $T = 500$ and $T = 1500$ respectively. In Figure 9 a seventh circle appears in the central vortex of the streamlines (associated with small negative values) corresponding to the contour value -0.11 which is unreacheable nor at $T = 275$ neither by the steady problem (actually, the eighth one if we count the distorted circle given by the *separation line*, with contour value -0.00001, that separates the secondary subvortices from the central one); we mention

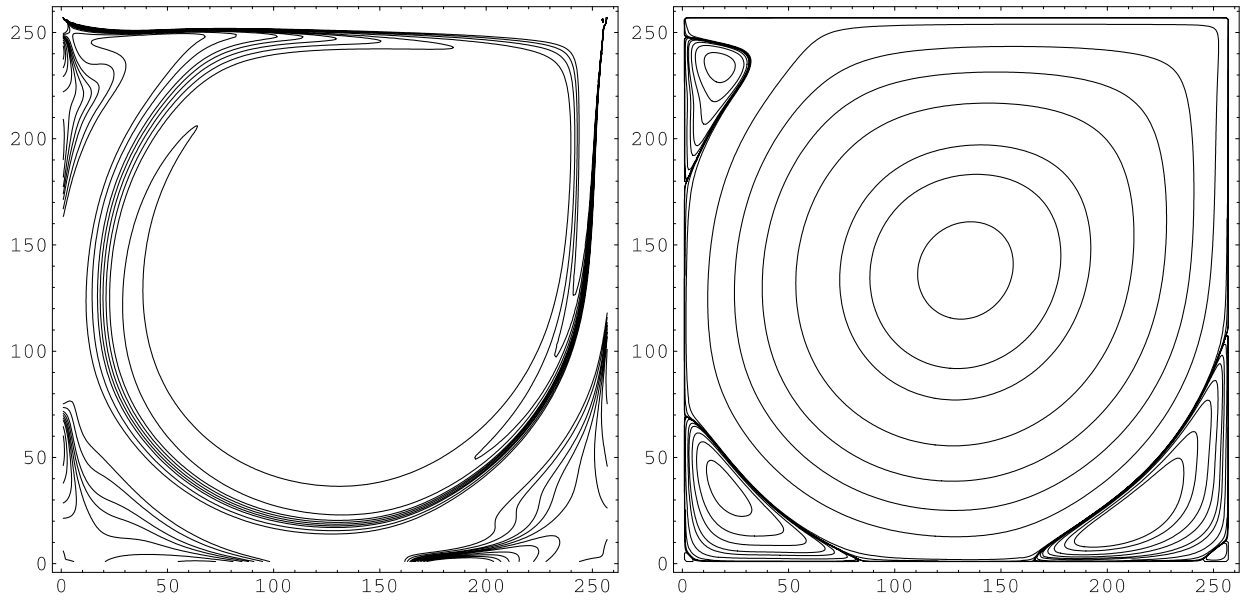

Figure 6 : Re=5000 (vs Goyon)

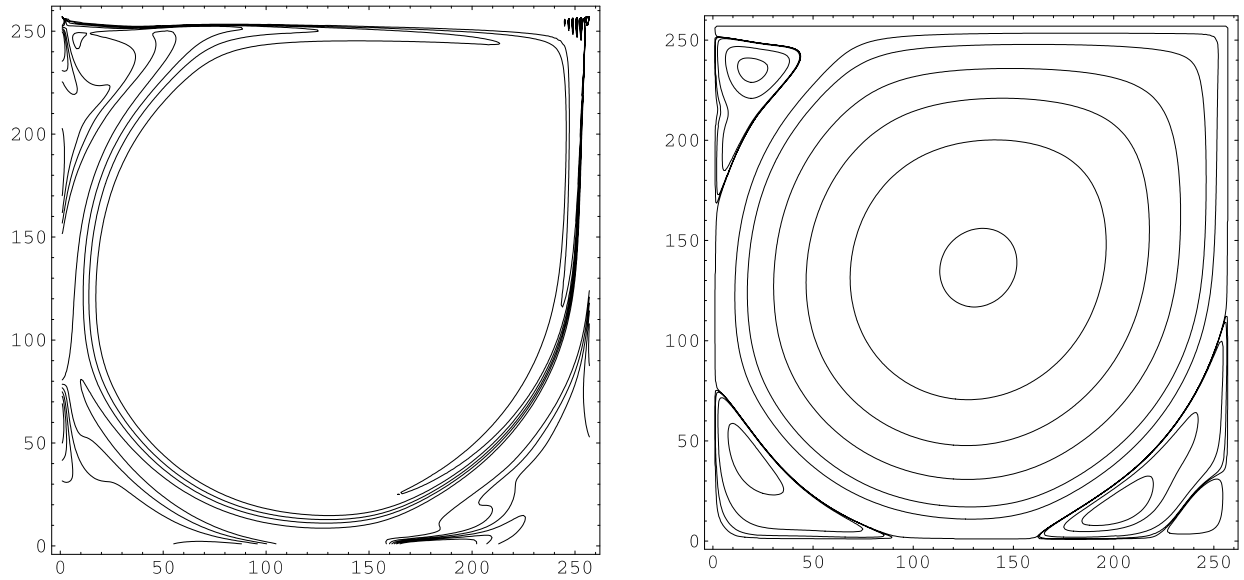

Figure 7 : Re=10000 at T=275 (almost S. & Keller steady problem)

in passing that this last contour value, -0.00001, gives rise to the tertiary subvortex in the right bottom corner too, which is moving clockwise like the central vortex. In Figure 10, several new things happen: the upstrean top secondary subvortex has been split into two ones but still being secondary subvortices since they correspond to small positive values and they are moving counter-clockwise, with the separation line in between. Thus, the number of subvortices has increased as time has elapsed. Moreover, the 3D graph of the stream function has enlarged negatively more; this being reflected in the appearance of two new small circles in the central vortex at smaller negative values, -0.113 and -0.1136 which definitely do not appear at $T = 500$ (as a consequence, the seventh circle at $T = 500$ has become bigger).

3). A set of results follows for $Re = 10000, 15000, 20000$ to show how the flow looks like close from its departure $t = 0$. We recall that for these flows $\Delta t = .0025$ too.

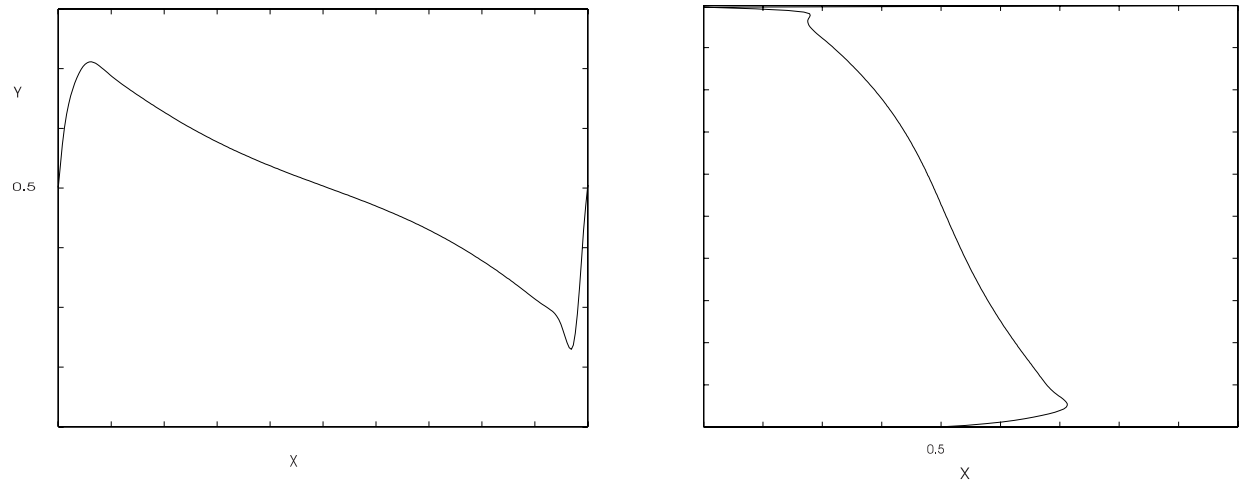

Figure 8 : Re=10000 (vs S. & Keller)

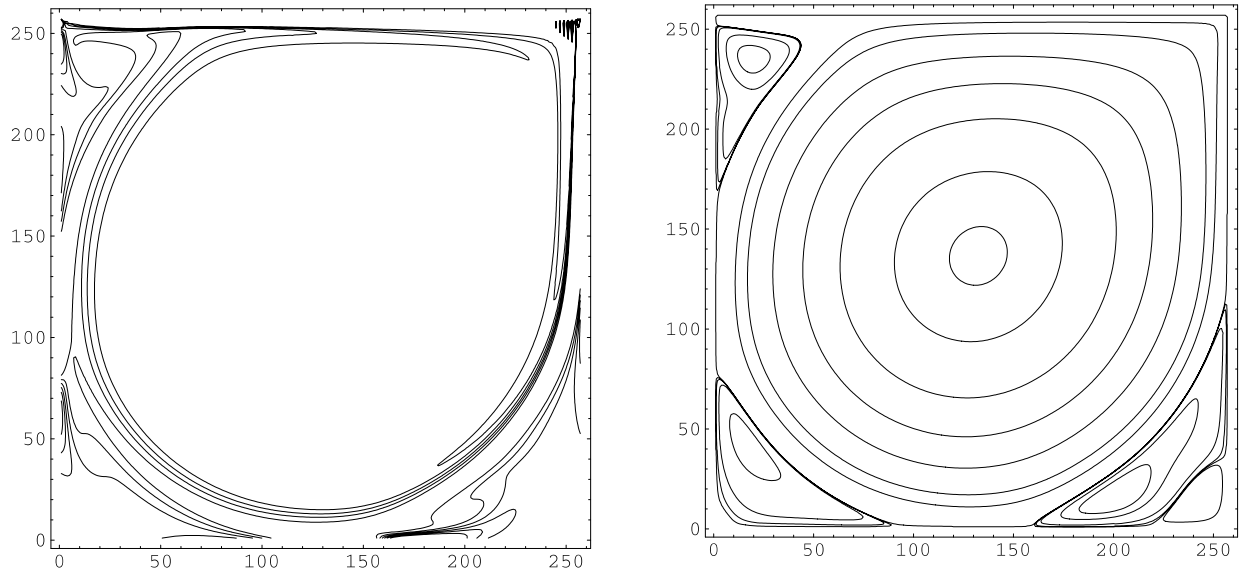

Figure 9 : Re=10000 at T=500

Figures 11, 12 and 13 show the flow at fixed final time $T = 25$ for Reynolds numbers $Re = 10000$ with $h = 1/256$, $Re = 15000$ with $h = 1/384$ and $Re = 20000$ with $h = 1/512$ respectively. The aim with these high Reynolds numbers is to show: a) the increase on the number of subvortices as the Reynolds number increases; b) the higher the Reynolds number the faster the movement of the center of the central vortex from down (left) to top (right) and then down again (clockwise) on the streamlines and, as can be observed, how such movement is also reflected in a similar way on the vorticity contours. It can also be pointed out that the small circle of the central vortex for $Re = 10000$ is obtained with the contour value -0.08 while the one of $Re = 15000$ and 20000 is obtained with -0.06; that is, the graph of the stream function for the smallest Reynolds number falls more than the others for higher ones.

On the other hand, for $Re = 10000$ fixed the number of subvortices increases as time increases, as can be observed on Figures 11, 9 and 10. Therefore, from this and 3.a) above, as pointed out in the Introduction, like in transition to turbulence (Landau and Lifshitz, 1989) the number of subvortices (or eddies) increases as either the Reynolds number or time increases.

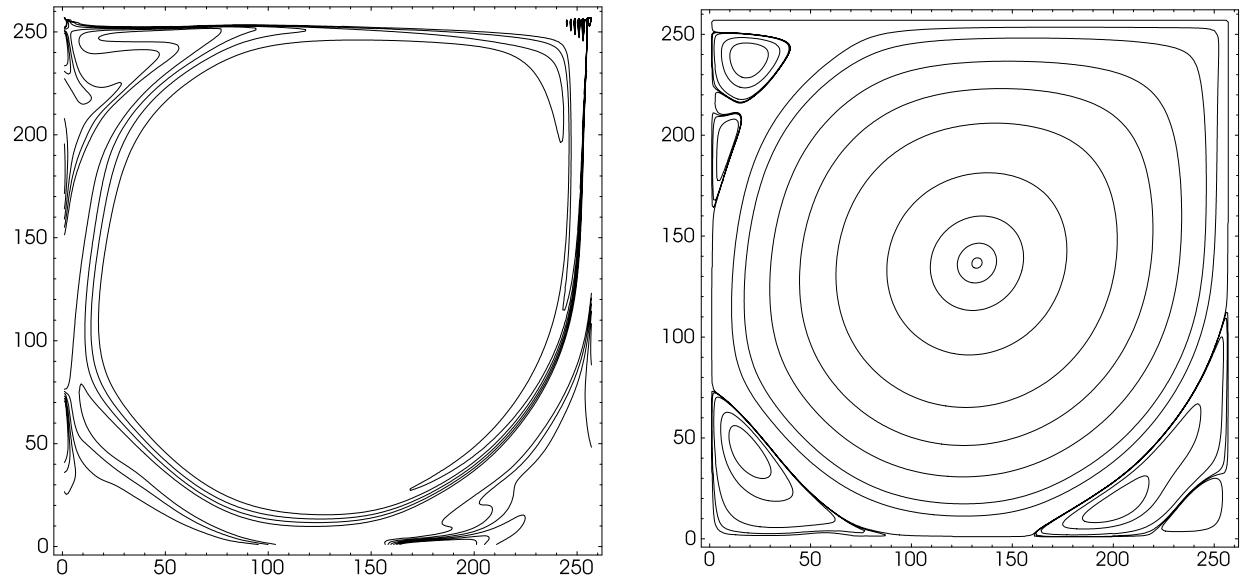

Figure 10 : Re=10000 at T=1500

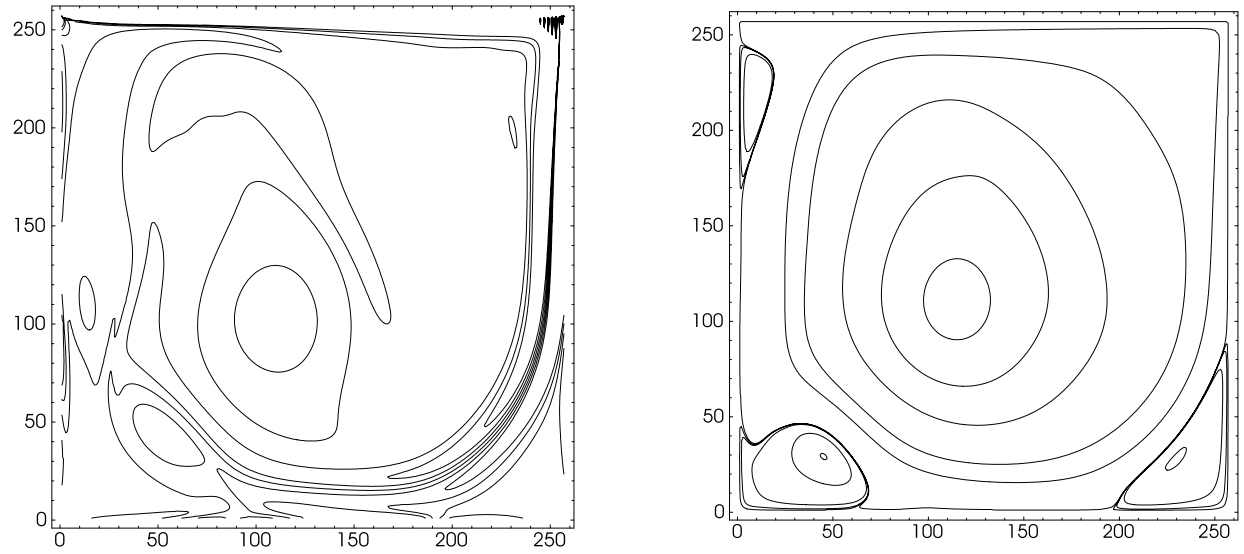

Figure 11 : Re=10000 at T=25

About the meshes for $Re \geq 10000$ we would like to say that for $Re = 10000$ we have chosen $h = 1/256$ because it reflects more likely the result of Schreiber and Keller from the steady problem (it is a kind of guide to obtain the right result, like the way we choose the right meshes to get the right flows for $400 \leq Re \leq 5000$). For $Re = 15000, 20000$ we have chosen those meshes to reach the physical meaning mentioned in 3.b) above, and to be consistent with 3.a), since that is what we expect as Re increases because the flow is faster for smaller viscosities, which is also in agreement for $Re = 10000$ with $h = 1/256$. Results for $Re = 15000$ and $Re = 20000$ were obtained with $h = 1/320$ and $h = 1/384$ respectively but they do not reflect such situation, at least not as clearly as the ones shown. We may say that in these cases we are choosing the "optimal" mesh based on physical grounds.

5 Conclusions

2D incompressible viscous flows up to Reynolds numbers $Re = 20000$ have been presented. These flows

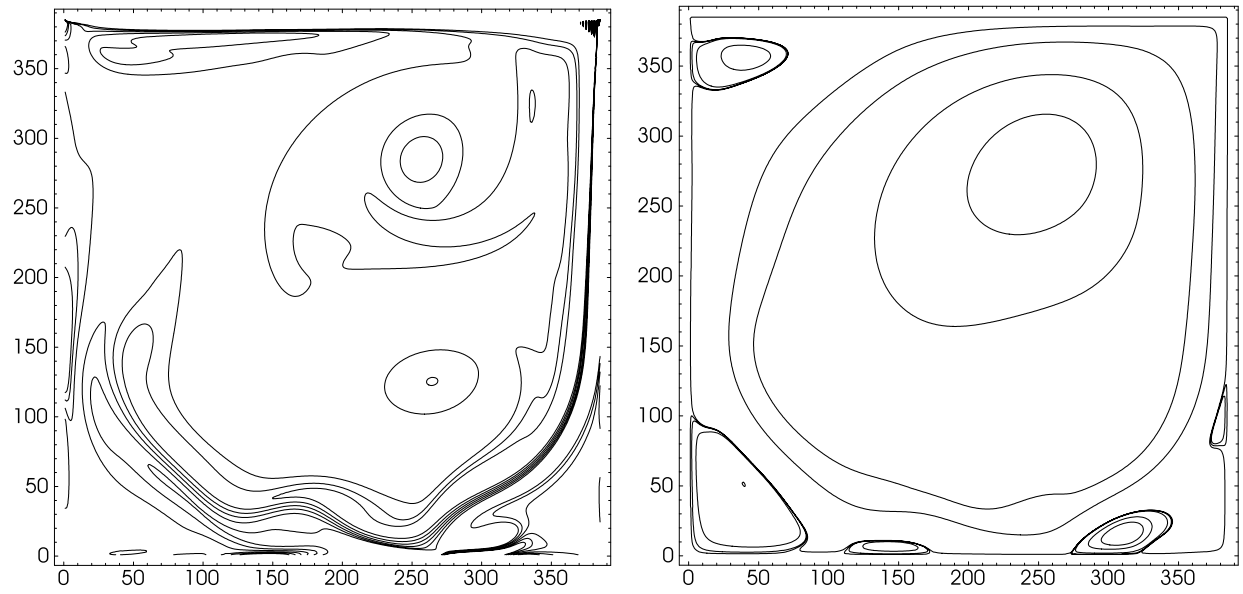

Figure 12 : Re=15000 at T=25

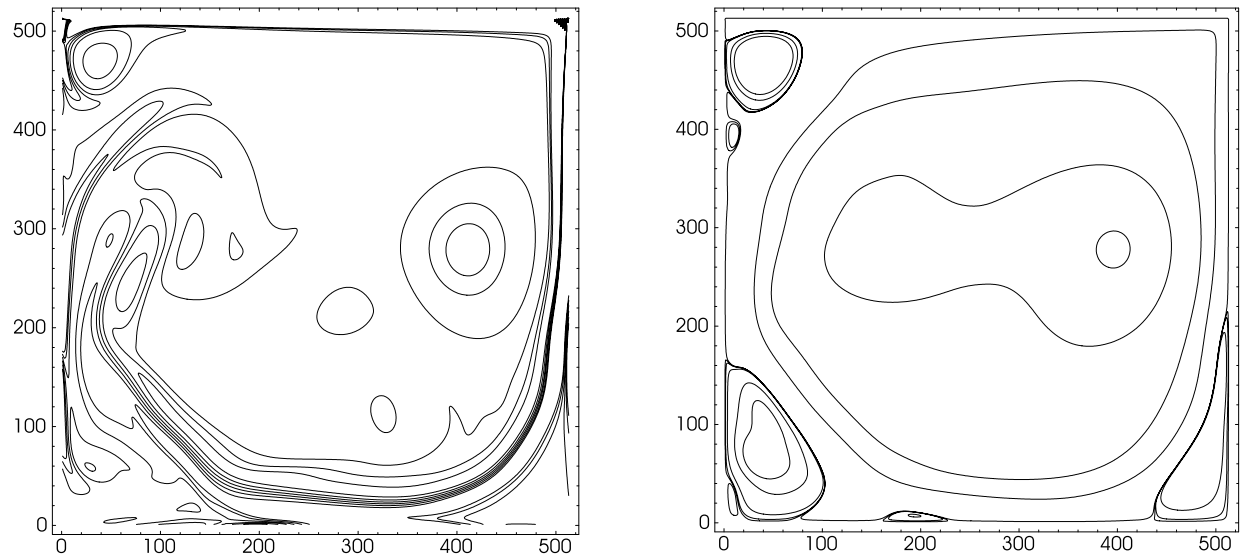

Figure 13 : Re=20000 at T=25

are obtained with a simple numerical procedure based mainly on a fixed point iterative process to solve the nonlinear elliptic system that results after time discretization on the unsteady Navier-Stokes equations in stream function-vorticity variables. The numerical procedure has already been proved to be good in capturing asymptotic steady states and computational experiments carried out so far indicate that it seems to be stable regardless of the value of the Reynolds number. Its simplicity allows us to get long time computations for some high Reynolds numbers as well as to see how the flow looks like close from its departure $t = 0$ for Reynolds numbers sufficiently larges. In addition, up to Reynolds numbers $Re = 10000$ the numerical procedure shows to be robust and fast enough to handle the associated memory demanding flow control problem in stream function-vorticity variables (Glowinski, 2003, Chapter X), which can lead to the control of turbulence, an important question for engineers (to either reduce or enhance it), Foias et al. (2001).

References

Adams, J.; Swarztrauber, P.; Sweet, R. (1980): FISHPACK: A Package of Fortran Subprograms for the Solution of Separable Elliptic PDE's, *The National Center for Atmospheric Research*, Boulder, Colorado, Usa.

Bermúdez, B.; Nicolás, A. (1999): An Operator Splitting Numerical Scheme for Thermal/Isothermal Incompressible Viscous Flows. *Int. J. Numer. Meth. Fluids*, 29, 397-410

Bruneau, C. H.; Jouron, C. (1990): An efficient scheme for solving steady incompressible Navier-Stokes equations. *J. Comput. Phys.* 389-413.

Dean, E. J.; Glowinski, R.; Pironneau, O. (1991): Iterative solution of the stream function-vorticity formulation of the Stokes problem, applications to the numerical simulation of incompressible viscous flow. *Comput. Methods Appl. Mech. Engrg.*, 87, 117-155

Doering, C. R.; Gibbon, J. D. (1995): Applied Analysis of the Navier-Stokes Equations. Cambridge University Press.

Foias, C.; Manley, O.; Rosa, R.; Temam, R. (2001): Navier-Stokes Equations and Turbulence. Cambridge University Press.

Glowinki, R. (2003): Hanbook of Numerical Analysis: Numerical Methods for Fluids (Part 3). North-Holland Ed.

Goyon, O. (1996): High-Reynolds number solutions of Navier-Stokes equations using incremental unknowns. *Comput. Methods Appl. Mech. Engrg.*, 130, 319-335

Gunzburger, M. D. (1989): Finite Element Methods for Viscous Incompressible Flows: A guide to theory, practice, and algorithms, Academic Press, INC.

Landau, L. D.; Lifshitz, E. M. (1989): *Fluid Mechanics*, second edition. Pergamon Press.

Lin, H.; Atluri, S. N. (2001): The Meshless Local Petrov Galerkin (MPLG) for Solving Incompressible Navier-Stokes Equations. *CMES: Computer Modelling in Engineering & Sciences*, Vol 2, No. 2,117-142

Pan, T. W.; Glowinski, R. (2000): A Projection/Wave-Like Equation Method for the Numerical Simulation of Incompressible Viscous Fluid Flow Modeled by the Navier-Stokes Equations. *Computational Fluid Dynamics Journal*, vol. 9, no. 2, 28-42

Peyret, R.; Taylor, T. D. (1983): Computational Methods for Fluid Flow. Springer-Verlag, New York.

Schreiber, R.; Keller, H. B. (1983): Driven cavity flow by efficient numerical techniques. *J. Comput. Phys.* 40, 310-333

Sweet, R. (1977): A cyclic reduction algorithm for solving block tridiagonal systems of arbitrary dimensions. **SIAM J. on Numer. Ana.**, 14, 706.

Tsai, C.; Young, D. L.; Cheng, A. H. (2002): Meshless BEM for Three-Dimensional Stokes Flows. *CMES: Computer Modeling in Engineering & Sciences*, Vol. 3, No. 1, 117-128